Influence of cold-stimulated adipocyte supernatant on the expression of adhesion-related molecules in Schwann cell line

Tiefeng Zhang [a], Yaxin Gan [a], Yulan Bai [a], Weijiang Hao [a], Ziqi Zeng [a], Feng Wu [a,**], Xianqi Li [a,b,*]

[a] Shanxi Medical University School and Hospital of Stomatology, Shanxi Province Key Laboratory of Oral Diseases Prevention and New Materials, Taiyuan, Shanxi, 030001, China
[b] Department of Oral and Maxillofacial Surgery, School of Dentistry, Matsumoto Dental University, Shiojiri, 399-0781, Japan

ARTICLE INFO

ABSTRACT

Bell's palsy is the most common form of facial nerve palsy. This study aimed to explore the pathogenesis of Bell's palsy by investigating the effect of cold-stimulated adipocyte supernatant on adhesion molecule expression in Schwann cell line. Schwann cells were cultured in regular or adipocyte-conditioned medium and analyzed using RNA sequencing. The mRNA expression of Schwann cell adhesion molecules melanoma cell adhesion molecule (MCAM), protocadherin 9 (PCDH9), and intercellular cell adhesion molecule 1 (ICAM1) was determined using real-time reverse-transcription polymerase chain reaction. Differentially expressed genes were identified, and Gene Ontology and Kyoto Encyclopedia of Genes and Genomes pathway enrichment analyses were conducted. Compared with Schwann cells in 37 °C, the expression of MCAM, PCDH9, and ICAM1 was downregulated in Schwann cells treated with cold-stimulated adipocyte supernatant compared with Schwann cells in 37 °C. Adipocytes subjected to cold exposure may weaken the adhesion capacity of Schwann cells and disrupt the local homeostasis of Schwann cell–axon interactions by affecting the expression of MCAM, PCDH9, and ICAM1, ultimately leading to the development of demyelinating lesions.

1. Introduction

Bell's palsy, also known as acute idiopathic peripheral facial nerve palsy, is the most common form of facial nerve palsy. Bell's palsy generally occurs in young adults, often manifested as the rapid onset of unilateral nerve palsy. Currently, the etiology of Bell's palsy is unknown [1]. Clinical studies have suggested that hypertension, diabetes [2,3], and the adverse cardiovascular and metabolic effects of obesity may increase the risk of Bell's palsy [4]. The epidemiology of Bell's palsy suggests that rapid changes in atmospheric pressure and environmental temperature may be the major risk factors [5–7]. The body is highly susceptible to Bell's palsy when in a state of fatigue and under alternating hot and cold stress [8].

Bell's palsy is an acute demyelinating disease, similar to Guillain–Barré syndrome [9,10]. The myelin sheath, a crucial structure of the peripheral nervous system, is formed by Schwann cells, a type of glial cell. Schwann cells form myelin sheaths by wrapping their plasma membranes in a spiral form around axons. The myelin sheath provides nutritional support to neurons and maintains the homeostasis of the neuronal microenvironment. This structure also enables rapid action potential conduction and facilitates complex Schwann cell–axon interactions [11,12]. The adhesion molecules on the Schwann cell surface play an important role in regulating intercellular interactions, signaling, and axonal regeneration [13]. The process of myelin formation in Schwann cells is regulated by multiple adhesion molecules. Schwann cells promote myelin formation by regulating neuregulin 1 signaling through the cell surface adhesion molecule E-cadherin [14]. Thus, myelin formation in Schwann cells is likely regulated by synergistic signaling events generated by multiple surface adhesion molecules.

The facial nerve network branches are mostly covered by subcutaneous fat, which possesses insulating properties that protect the organism from damage caused by hot and cold stresses. White adipocyte tissue, as an active endocrine organ, releases adipocytokines through specific intercellular signaling pathways. This mechanism keeps peripheral nerves in a healthy, repairable state and maintains the innervation of target tissues [15,16]. As facial cold exposure is a risk factor for Bell's palsy, the development of Bell's palsy is associated with metabolic

Abbreviations

ADSC	adipose derived mesenchymal stem cell
ADIPO CM	adipocyte conditioned medium
BDNF	brain-derived neurotrophic factor
BP	biological process
CAM	cell adhesion molecule
CC	cellular component
DEG	differentially expressed gene
DM	differentiation medium
FBS	fetal bovine serum
GO	Gene Ontology
ICAM1	intercellular cell adhesion molecule 1
IGSF	immunoglobulin superfamily
KEGG	Kyoto Encyclopedia of Genes and Genomes
L-DMEM	Dulbecco's modified Eagle's medium with low glucose
MAPK	mitogen-activated protein kinase
MAPKK	MAPK kinase
MAPKKK	MAPK kinase kinase
MCAM	melanoma cell adhesion molecule
MF	molecular function
NGF	nerve growth factor
PCDH9	protocadherin 9
RNA-Seq	RNA sequencing
RT-qPCR	real-time reverse-transcription polymerase chain reaction

Table 1
RT-qPCR primer sequences.

Gene	Forward (5' to 3')	Reverse (3' to 5')
MCAM	GTCCTCACAGCAGAGCCAACAG	ACAGCAAGCACCAGCGTACATAC
PCDH9	CCTGGTTCCGTGGTTGCTGAAG	TCCTTTGTTGTTCCCGCTCACTATG
ICAM1	CCTGGTCCTCCAATGGCTTCAAC	TCTGTGGGATGGATGGATACCTGAG
ACTB	TGTCACCAACTGGGACGATA	GGGGTGTTGAAGGTCTCAAA

MCAM: melanoma cell adhesion molecule; PCDH9: protocadherin 9; ICAM1: intercellular cell adhesion molecule-1; ACTB: actin b.
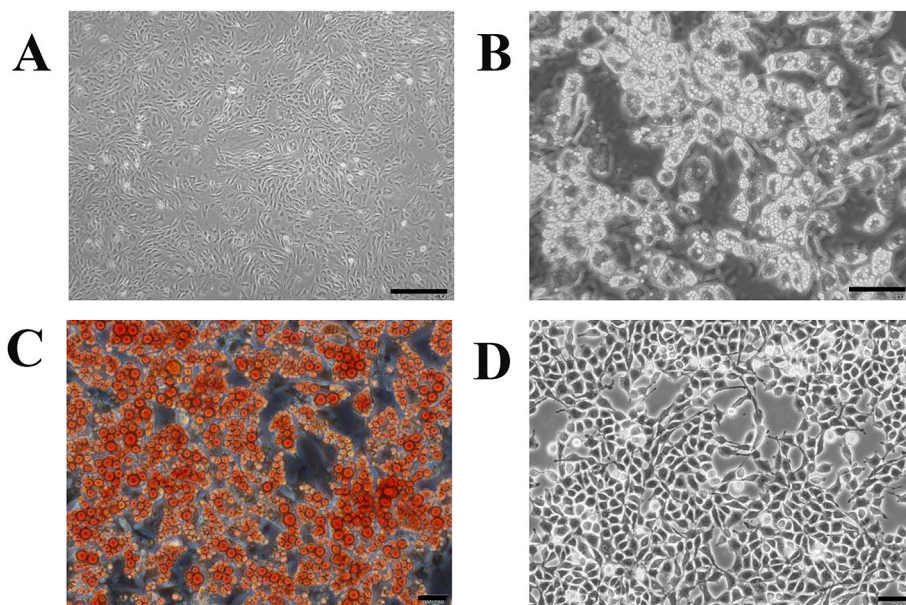
Fig. 1. Adipose tissue-derived mesenchymal stem cells (ADSCs), adipocytes, and Schwann cells. (A) ADSCs were long, spindle-shaped, and locally fused in a swirling pattern. Scale bar: 500 μm. (B) Differentiation of ADSCs into adipocytes was induced. Adipocytes appeared as round lipid droplets of varying sizes. With time, the lipid droplets slowly fused, and the cell morphology gradually became round. Scale bar: 100 μm. (C) Red staining of round lipid droplets indicated the presence of mature adipocytes. Scale bar: 100 μm. (D) Schwann cells were small and either round or long and shuttle-shaped. Scale bar: 100 μm. (For interpretation of the references to colour in this figure legend, the reader is referred to the Web version of this article.)

Table 2
Quality Control of four groups.

|	Total reads	Total mapped	Multiple mapped	Uniquely mapped	Reads mapped in proper pairs
37 DMEM group;	37239366 (100.00%)	35402339 (95.07%)	3292058 (8.84%)	32110281 (86.23%)	29435944 (79.05%)
37 ADIPO CM group	39759838 (100.00%)	37886183 (95.29%)	3408170 (8.57%)	34478013 (86.72%)	31644910 (79.59%)
30 ADIPO CM group	36095536 (100.00%)	35216015 (97.56%)	3072554 (8.51%)	32143461 (89.05%)	30636468 (84.88%)
30 DMEM group	39627522 (100.00%)	37541276 (94.74%)	3428632 (8.65%)	34112644 (86.08%)	31194778 (78.72%)

and inflammatory changes in subcutaneous adipose tissue. Cold exposure can cause the upregulation of inflammatory chemokines in adipocytes [17]. However, whether changes in Schwann cell microenvironment resulting from the effects of cold exposure on adipocytes alter Schwann cell function, is not known.

In this study, the cells in the mild-hypothermia group were exposed to a temperature of 30 °C. This temperature was selected based on pre-experimental grouping. In addition, 30 °C is a critical point in
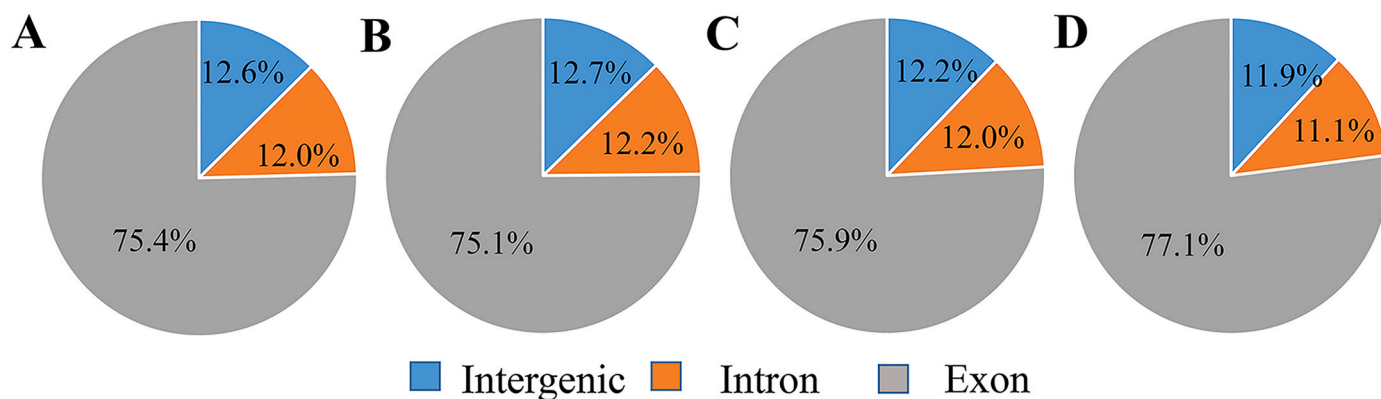
Fig. 2. Pie chart of reads mapped to each genomic region. The pie chart represents the proportion of reads mapped to exons (Exon), introns (Intron), and intergenic regions (Intergenic), as determined by comparing the reads to the reference genome. (A) 37 DMEM group; (B) 37 ADIPO CM group; (C) 30 ADIPO CM group; (D) 30 DMEM group.
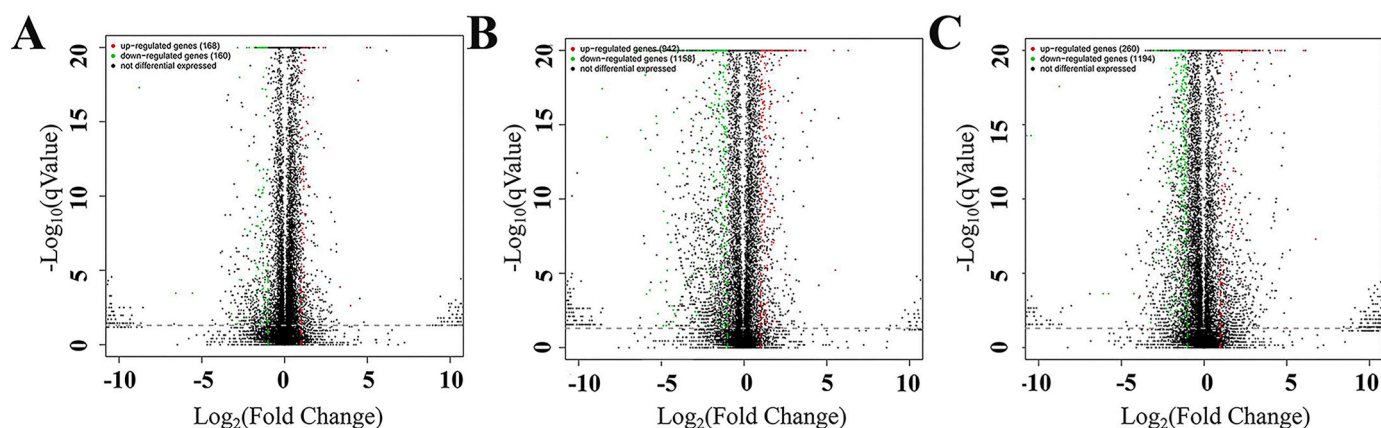

Fig. 3. Volcano plots depicting expression differences. Each point on the graph represents a gene. Red indicates upregulation, green indicates downregulation, and black indicates non-differential expression. (A) 37 ADIPO CM vs. 37 DMEM groups; (B) 30 ADIPO CM vs. 37 DMEM groups; (C) 30 DMEM vs. 37 DMEM groups. (For interpretation of the references to colour in this figure legend, the reader is referred to the Web version of this article.)
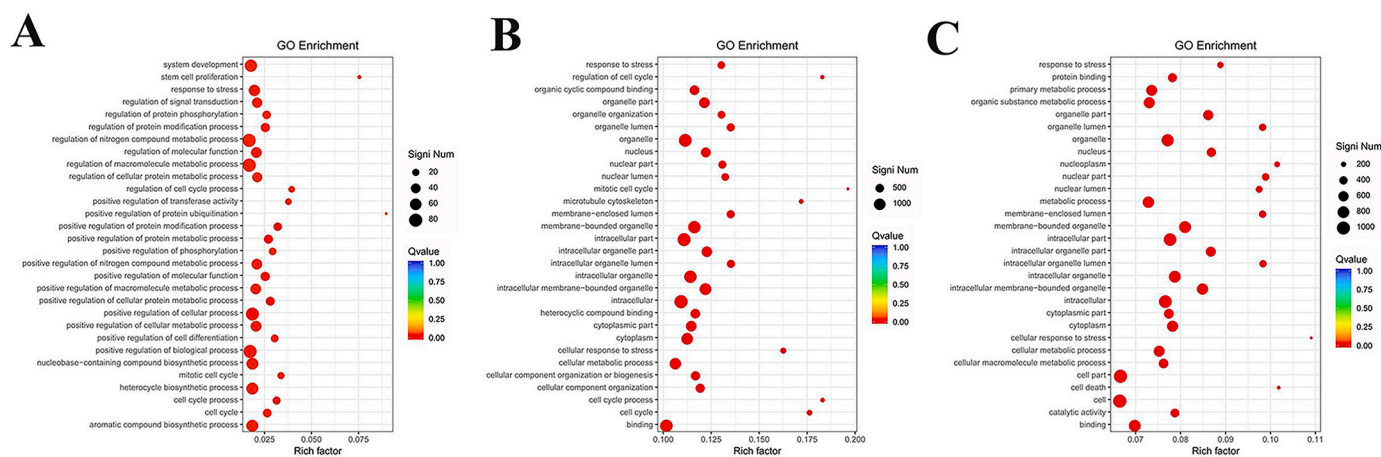
Fig. 4. Scatter plot of significantly enriched functions. The top 30 most significantly enriched Gene Ontology (GO) terms were selected to establish the scatter plot. (A) 37 ADIPO CM vs. 37 DMEM groups; (B) 30 ADIPO CM vs. 37 DMEM groups; (C) 30 DMEM vs. 37 DMEM groups.

temperature grading, as this point allows the temperature around the facial nerves to remain relatively stable despite changes in ambient temperature, owing to the protective effects of facial adipose tissue [17]. We investigated how adipocytes subjected to cold exposure affect the expression profile of adhesion molecules in Schwann cells, in order to

provide new insights into the etiology of Bell's palsy.
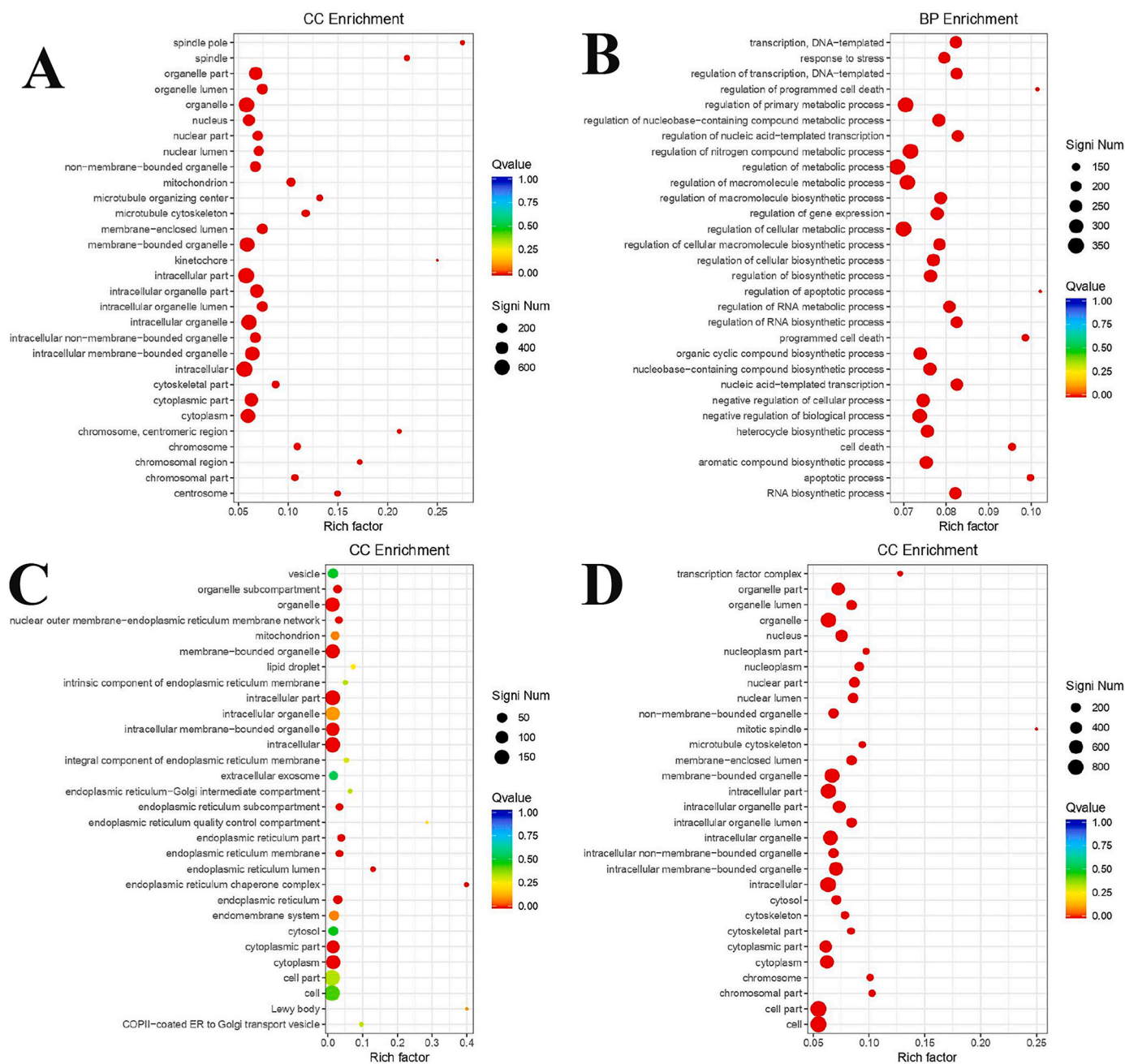
Fig. 5. Scatter plot of significantly enriched functions. The top 30 most significantly upregulated or downregulated differentially expressed gene (DEG)-enriched Gene Ontology (GO) terms were selected to establish the scatter plot. (A) 30 ADIPO CM vs. 37 DMEM upregulated DEGs in cellular components (CC) terms; (B) 30 DMEM vs. 37 DMEM upregulated DEGs in CC terms; (C) 30 ADIPO CM vs. 37 DMEM downregulated DEGs in BP terms; (D) 30 DMEM vs. 37 DMEM downregulated DEGs in CC terms.

Table 3
KEGG pathway analysis of DEGs in 37 ADIPO CM group.

id	Description	Qvalue	cold-exposed genes
ko04668	TNF signaling pathway	0.0005	Cxcl1
ko04060	Cytokine-cytokine receptor interaction	0.0213	Tnfsf18,Cxcl1,Tslp

KEGG: Kyoto Encyclopedia of Genes and Genomes.

2. Material and methods

2.1. Animals

Adipose tissue-derived mesenchymal stem cells (ADSCs) were obtained from 4-week-old male Sprague–Dawley (SD) rats at the Animal Center of Shanxi Medical University. As male SD rats have more adipose tissue than females, males were selected as the experimental animals. The rats were maintained at 25 ± 2 °C under a 12 h light/12 h dark cycle. The experiment involved six male SD rats, each weighing 100–200 g. The experimental design was approved by the Animal Experimentation Committee of the Stomatological Hospital of Shanxi Medical University (No. 2017007). All animal experiments complied

Table 4
KEGG pathway analysis of DEGs in 30 ADIPO CM group.

id	Description	Qvalue	cold-exposed genes
ko04668	TNF signaling pathway	0.0010	Ifi47,Icam1,Edn1,Creb3l1,Fos, Cxcl10,Pik3r3,Cxcl1,Ptgs2
ko03410	Base excision repair	0.0010	Pole2,Xrcc1,Parp2,Mutyh
ko00970	Aminoacyl-tRNA biosynthesis	0.0012	Tars2,Sepsecs, Aars2,Pars2,Dars2
ko03420	Nucleotide excision repair	0.0015	Rad23a,Pole2,Cul4a
ko03440	Homologous recombination	0.0019	Rad54b,Rad52,Rad51b
ko04068	FoxO signaling pathway	0.0023	Plk2,Gadd45a,Plk1,Ccnb1,Sod2, Bcl6,Klf2,Pik3r3,Tgfb3,Tgfb2, Gadd45b,Tnfsf10
ko00640	Propanoate metabolism	0.0033	Suclg2,Echs1,LOC100911186, Pccb
ko04978	Mineral absorption	0.0064	Hmox1,RGD1566189, RGD1560687,Ftl1l1
ko04380	Osteoclast differentiation	0.0064	Sqstm1,Stat2,Ppp3cb,Fos,Pik3r3, Irf9,LOC108348047,Socs1,Tgfb2
ko04110	Cell cycle	0.0087	Cdc20,Gadd45a,Plk1,Ccnb1,Cdk1, Pttg1,Bub1b,Cdc14a,E2f5,Atr, Tgfb3,Tgfb2,Gadd45b,Orc3
ko03030	DNA replication	0.0090	Pole2
ko01212	Fatty acid metabolism	0.0134	Acadl, Mecr,Echs1, LOC100911186
ko00760	Nicotinate and nicotinamide metabolism	0.0134	Enpp1,Nadk2,Cd38
ko00071	Fatty acid degradation	0.0161	Acadl, Echs1,LOC100911186
ko04623	Cytosolic DNA-sensing pathway	0.0163	Irf7,Ddx58,Il33,Cxcl10,Zbp1
ko04622	RIG-I-like receptor signaling pathway	0.0193	Isg15,Irf7,Trim25,Ifih1,Tbkbp1, Ddx58,Cxcl10,Dhx58,Nlrx1
ko04146	Peroxisome	0.0199	Idh2,Gnpat,Hsd17b4
ko04115	p53 signaling pathway	0.0235	Thbs1,Gadd45a,Ccnb1,Cdk1,Atr, Gadd45b,Serpine1
ko04141	Protein processing in endoplasmic reticulum	0.0245	Calr,Hsp90b1,Ppp1r15a,Eif2ak2, Dnajc3,Rnf185,Rad23a,Hspa1b, Hspa1a,Eif2ak4
ko04010	MAPK signaling pathway	0.0245	Hspb1,Gadd45a,Rasgrp3,Mras, Ppp3cb,Hspa1b,Dusp10,Hspa1a, Bdnf,Fos,Tgfb3,Map3k4,Tgfb2, Gadd45b,Cacng7,Ngf
ko04620	Toll-like receptor signaling pathway	0.0317	Irf7,Fos,Cxcl10,Pik3r3,Tlr6
ko04144	Endocytosis	0.0332	Pml,Hspa1b,RT1-CE4,Hspa1a, Tgfb3,Rab11fip1,Tgfb2,RT1-S3, Grk5
ko03460	Fanconi anemia pathway	0.0407	Fancd2,Atr,Rmi2
ko04612	Antigen processing and presentation	0.0410	Calr,Tap1,Hspa1b,RT1-CE4, Hspa1a,RT1-S3
ko00240	Pyrimidine metabolism	0.0442	Tk1,Cmpk2,Dut,Pole2
ko01200	Carbon metabolism	0.0468	Idh2,Suclg2,Adpgk, Pfkm,Echs1, LOC100911186,Pccb
ko00600	Sphingolipid metabolism	0.0477	Sphk1,Gba,Sgms2
ko00280	Valine, leucine and isoleucine degradation	0.0485	Echs1,LOC100911186,Pccb, Mccc2

Table 5
KEGG pathway analysis of DEGs in 30 DMEM group.

id	Description	Qvalue	cold-exposed genes
ko04141	Protein processing in endoplasmic reticulum	0.0000	Hspa5,Hyou1,Pdia4,Sel1l, Ero1b
ko04141	Protein processing in endoplasmic reticulum	0.0011	Hspa5,Hyou1,Pdia4,Hsph1, Dnaja1,Sel1l,Ero1b,Preb, Hspa1a
ko04070	Phosphatidylinositol signaling system	0.0012	Tmem55a,Itpr1,Pip5k1b
ko00520	Amino sugar and nucleotide sugar metabolism	0.0014	Gmppb, Gnpnat1
ko00562	Inositol phosphate metabolism	0.0088	Pip5k1b
ko03460	Fanconi anemia pathway	0.0214	Rad51,Palb2

Table 6
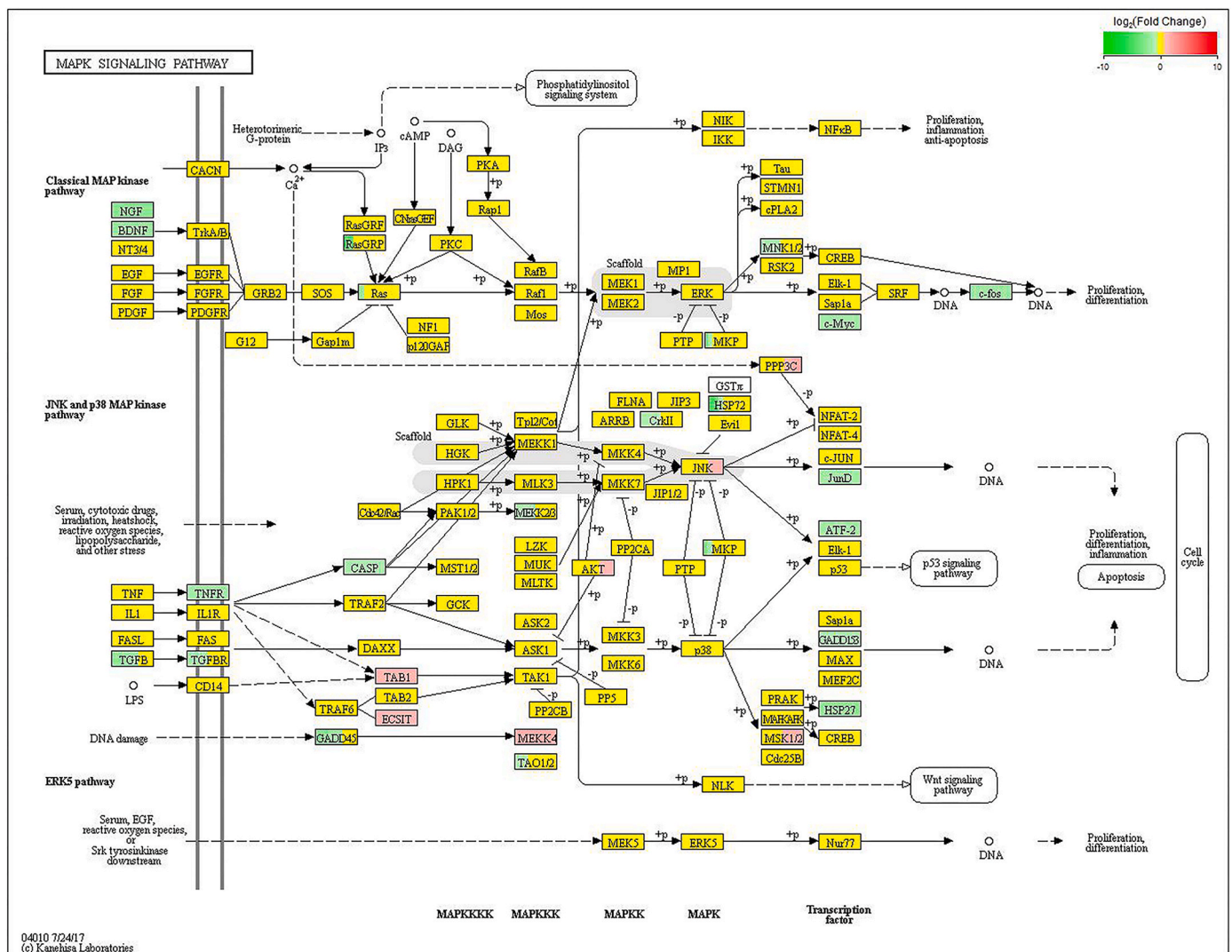KEGG pathway enrichment analysis in the 30 ADIPO CM group.

Class	KEGG pathway
metabolism	ko01200; ko01212; ko00280; ko00600; ko00071; ko00240; ko00760; ko00640
genetic information processing	ko03410; ko03420; ko03440; ko03030; ko04141; ko03460; ko00970
organismal systems	ko04620; ko04978; ko04380; ko04623; ko04622; ko04612
cellular processes	ko04144; ko04110; ko04146; ko04115
environmental information processing	ko04010; ko04068; ko04668

transferred to a Petri dish containing phosphate-buffered saline. To obtain pure white adipose tissue, blood vessels, muscle and other impurities were carefully removed.

White adipose tissue was minced and digested in 0.2% collagenase type I solution at 37 °C for 50–60 min. The separated ADSCs were resuspended in Dulbecco's modified Eagle's medium with low glucose (L-DMEM; PYG0072, Boster Bio), supplemented with 10% fetal bovine serum (FBS; 0510, ScienCell) and 1% penicillin/streptomycin/amphotericin B solution. When the third generation of ADSCs reached full confluence, the ADSCs were stimulated with differentiation medium (DM) containing L-DMEM supplemented with 10% FBS, 1% penicillin/streptomycin/amphotericin B sterile solution, 1 μM dexamethasone (D6040-100, Sigma), 200 μM indomethacin (I8280-5, Solarbio), 0.5 mM IBMX (I8450, Solarbio), and 10 μM insulin (I8040-25, Solarbio) for 4 days. The cells were then maintained in DM containing only 10 μM insulin, L-DMEM supplemented with 10% FBS, and 1% penicillin/streptomycin/amphotericin B sterile solution. Mature adipocytes were identified using Oil Red O staining. The adipocytes were then randomly divided into two groups (maintained at 37 °C and 30 °C, respectively). Each group was cultured in serum-free DMEM at 37 °C or 30 °C for 8 h. Thereafter, the cell supernatants were extracted and mixed with DMEM at a 1:1 ratio to produce 37 °C adipose-conditioned medium (37 ADIPO CM) and 30 °C adipose-conditioned medium (30 ADIPO CM), respectively.

2.3. Schwann cell culture

Rat Schwann cell line (RSC-96) were obtained from the Institute of Basic Medical Sciences, Chinese Academy of Medical Sciences. Schwann cells were cultured in medium with or without adipocyte conditioning. When the cells grew to 80–90% confluence for passaging, all cells were maintained at 37 °C in a humidified 5% CO_2 atmosphere. The number of cells inoculated in each T25 culture medium at the time of passaging was 10^4. The third generation of Schwann cells was used for follow-up experiments. Four groups were established: the 37 DMEM group (37 °C in DMEM medium), 37 ADIPO CM group, 30 ADIPO CM group, and 30 DMEM group (30 °C in DMEM medium). The 37 DMEM and 37 ADIPO CM groups were incubated at 37 °C for 8 h, and the 30 ADIPO CM and 30

with the ARRIVE guidelines.

2.2. Adipocyte culture

All instruments were sterilized in a high-temperature autoclave prior to use. SD rats were anesthetized with 150 mg/kg of sodium pentobarbital, and necropsy was performed to ensure the death of all rats. Cardiac and respiratory arrest, muscle relaxation, and lack of reflexes were considered as signs of death. SD rats were submerged in 75% ethanol for 10 min, after which the abdominal skin was cut on ice. White adipose tissue was separated from the groin using ophthalmic scissors and

Fig. 6. Kyoto Encyclopedia of Genes and Genomes pathway analysis. "Mitogen-activated protein kinase signaling pathway" (ko04010) enrichment was repressed (q < 0.05) in Schwann cells treated with cold-stimulated adipocyte supernatant.

DMEM groups were incubated at 30 °C for 8 h. Next, the cells were harvested for RNA extraction and RNA sequencing (RNA-Seq).

2.4. RNA extraction and quality control

The cells were collected after 8 h of culture. A total RNA extractor (Sangon Biotech (Shanghai) Co., Ltd., Shanghai, China) was used for total RNA extraction according to the manufacturer's protocol. The Qubit® 2.0 Fluorometer (Q32866, Invitrogen, MA, USA) was used to measure RNA concentration, and purity was measured by determining the A260/A280 ratio.

### 2.5. cDNA library construction and RNA-Seq

One microgram of RNA per sample was used for mRNA sequencing library preparation. The mRNA in each sample was enriched using oligo (dT) magnetic beads and fragmented with fragmentation buffer (approximately 200 bp). mRNA libraries were created using the Hieff NGS™ MaxUp Dual-mode mRNA Library Prep Kit for Illumina® (12301ES96, Yeasen Biotechnology (Shanghai) Co., Ltd., Shanghai, China) following the manufacturer's protocols. Libraries for paired-end sequencing were prepared (PE150; sequencing reads, 150 bp) at Sangon Biotech (Shanghai) Co., Ltd., using the MGISEQ-2000 platform.

2.6. Identification of differentially expressed genes

Data processing was performed using Trimmomatic. Valid data were mapped to the genome using HISAT2, and clean reads were obtained. Differentially expressed genes (DEGs) were identified using the following screening criteria: |$\log_2$ (Fold Change) | > 1 and q-value (adjusted p-value) < 0.05.

2.7. Gene Ontology and Kyoto Encyclopedia of Genes and Genomes enrichment analyses

Gene Ontology (GO) annotations are divided into three major categories: molecular functions (MFs), biological processes (BPs), and cellular components (CCs). The Kyoto Encyclopedia of Genes and Genomes (KEGG), commonly used for pathway analysis, is a comprehensive database that integrates genomic, chemical, and systemic functional information. All DEGs were subjected to GO functional enrichment analysis, using the public GO database (http://geneontology.org/). DEGs with a q-value of <0.05 were subjected to KEGG pathway enrichment analysis (http://www.kegg.jp). GO enrichment analysis and KEGG pathway enrichment analysis were performed using topGO v2.24.0 software and clusterProfiler v3.0.5, respectively.
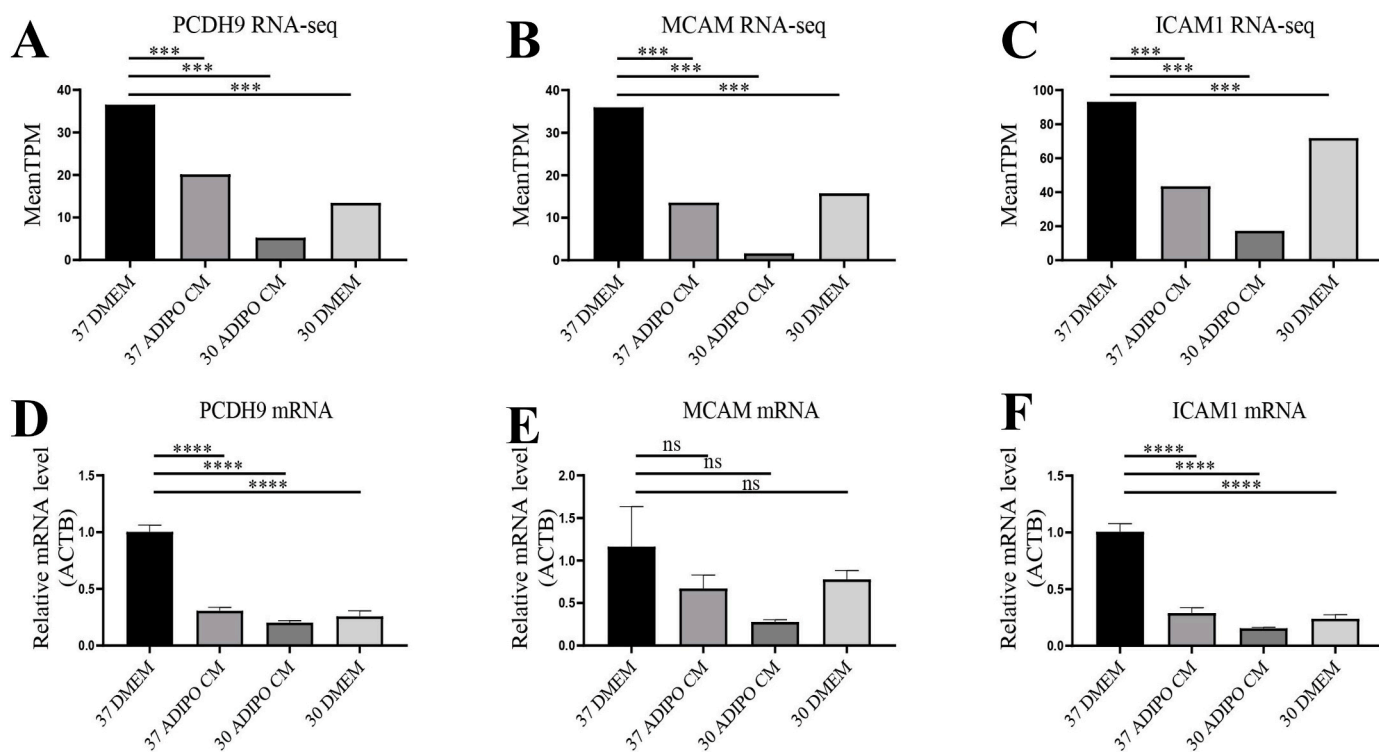
Fig. 7. Quantitative reverse transcription-polymerase chain reaction (RT-qPCR) validation of RNA sequencing (RNA-Seq) data. (A, B, C) RNA-Seq of PCDH9, MCAM, and ICAM1, respectively, in 37 ADIPO CM vs. 37 DMEM groups; 30 ADIPO CM vs. 37 DMEM groups; and 30 DMEM vs. 37 DMEM groups. All p-values were <0.001. (D) RT-qPCR results of PCDH9 in 37 ADIPO CM vs. 37 DMEM groups, $p < 0.0001$; 30 ADIPO CM vs. 37 DMEM groups, $p < 0.0001$; 30 DMEM vs. 37 DMEM groups, $p < 0.0001$. (E) RT-qPCR of MCAM in 37 ADIPO CM vs. 37 DMEM groups, $p = 0.4324$; 30 ADIPO CM vs. 37 DMEM groups, $p = 0.0936$; 30 DMEM vs. 37 DMEM groups, $p = 0.6042$; (F) RT-qPCR results of ICAM1 in 37 ADIPO CM vs. 37 DMEM groups, $p < 0.0001$; 30 ADIPO CM vs. 37 DMEM groups, $p < 0.0001$; 30 DMEM vs. 37 DMEM groups, $p < 0.0001$. * represents a comparison between the treated and control groups, *: $p < 0.05$, **: $p < 0.01$, ***: $p < 0.001$, ****: $p < 0.0001$; ns: no significant differences. PCDH9: Protocadherin 9; MCAM: Melanoma Cell Adhesion Molecule; ICAM1: Intercellular Adhesion Molecule 1.

2.8. Real-time reverse-transcription polymerase chain reaction

Real-time reverse-transcription polymerase chain reaction (RT-qPCR) was used to verify the accuracy of the mRNA expression profiles [18]. Total RNA was extracted from Schwann cells using a total RNA extraction reagent (TRIgent, MF034-01, Mei5bio; Science & Technology Co., Ltd., Beijing, China). The RNA concentration was diluted to 250 ng/μl. Next, 500 ng of each RNA sample was reverse-transcribed into cDNA using a reverse transcription kit (MF166-01, Mei5bio; Science & Technology Co., Ltd.). Reaction conditions were as follows: 42 °C for 15 min, followed by 50 °C for 5 min, 96 °C for 5 min, and a final holding temperature of 4 °C. RT-qPCR analysis was performed via QuantStudio™ (A40426; Thermo Fisher Scientific, MA, USA), using the SYBR Green qPCR Mix (MF797-05, Mei5bio; Science & Technology Co., Ltd.). Primer sequences were designed based on the coding sequence of the target genes obtained from the NCBI database (https://www.ncbi.nlm.nih.gov/) (Table 1). The RT-qPCR program was as follows: an initial 95 °C denaturation step for 30 s, followed by 40 cycles at 95 °C for 15 s, 60.5 °C for 15 s, and 72 °C for 30 s. The experimental RT-qPCR data were normalized using β-actin expression as an internal reference. Three technical replicates and three biological replicates were established for each sample, and the experimental results were quantified using the $2^{-\Delta\Delta Ct}$ method [18]. RT-qPCR analysis of differentially expressed genes was used to validate the RNA-Seq data.

2.9. Statistical analysis

The correlations between the RNA-Seq data and RT-qPCR data were analyzed using GraphPad Prism v8.00. The RT-qPCR data are presented as mean ± standard deviation (n = 3). A one-way ANOVA was used for multiple group comparisons, and a *t*-test was used for two-group comparisons. Dunnett's test was employed as the post hoc test following one-way ANOVA. Results with P < 0.05 were considered statistically significant.

3. Results

3.1. Confirmation of differentiation into mature adipocytes and Schwann cell morphology

Inguinal white adipose tissue collected from SD rats was digested to obtain ADSCs. The ADSCs exhibited a spindle-shaped morphology, which is characteristic of fibroblasts (Fig. 1A). After 8 days of induction, the formation of round lipid droplets was clearly visible (Fig. 1B). One hour after Oil Red O staining, the lipid droplets appeared red when 60% isopropanol was added (Fig. 1C), confirming successful differentiation into mature adipocytes. The Schwann cells were small and either round or long and shuttle-shaped (Fig. 1D).

3.2. RNA-Seq data

High-quality total RNA (A260/A280 > 1.8) was obtained from cultured cells. RNA-Seq generated four raw sequences (Table 2). The coverage of each transcript at each position was calculated by comparing the results. In all four groups of samples, the proportion of reads mapping to the exonic regions was more than 75% (Fig. 2). These results confirmed the quality and reliability of the sequencing data.

3.3. Identification and analysis of DEGs

After RNA-Seq, 328 DEGs (168 upregulated and 160 downregulated) (Fig. 3A), 2100 DEGs (942 upregulated and 1158 downregulated) (Figs. 3B), and 1454 DEGs (260 upregulated and 1194 downregulated) (Fig. 3C) were identified in the 37 ADIPO CM group, 30 ADIPO CM group, and 30 DMEM group, respectively, compared with those in the 37 DMEM group (Fig. 3).

3.4. GO enrichment analysis and KEGG enrichment analysis

Following GO analysis of all DEGs, top 30 most significantly enriched GO entries were selected, and a functional scatter plot was generated (Fig. 4). Compared to the 37 DMEM group, the 37 ADIPO CM group showed the most enrichment in genes related to "response to stress" and "regulation of macromolecule metabolic process" (Fig. 4A), whereas the 30 ADIPO CM group showed significant enrichment in GO entries related to "organelle" and "binding" (Fig. 4B), and the most significantly enriched GO entries in the 30 DMEM group included "cell part" and "binding" (Fig. 4C).

The GO enrichment analysis showed that in the 30 ADIPO CM group, significantly upregulated DEGs were mainly enriched in CC terms, including "organelle" and "intracellular" (Fig. 5A), whereas significantly downregulated DEGs were mainly enriched in BP terms, including "cell death" and "regulation of gene expression" (Fig. 5B). This finding indicates that the DEGs in this group were mainly associated with BPs and CCs. In the 30 DMEM group, significantly upregulated DEGs were mainly enriched in CC terms, including "cytoplasm" and "intracellular" (Fig. 5C), while significantly downregulated DEGs in this group were mainly enriched in CC terms, including "cell part" and "organelle" (Fig. 5D). In the 37 ADIPO CM group, significantly downregulated DEGs were mainly enriched in BP terms.

The KEGG pathway enrichment analysis showed that "protein processing in endoplasmic reticulum" (ko04141) was the most significantly enriched pathway in the 30 DMEM group, whereas in the 37 ADIPO CM and 30 ADIPO CM groups, the "TNF signaling pathway" (ko04668) was the most significantly enriched pathway (Tables 3–5).

In the 30 ADIPO CM group, the KEGG pathway enrichment analysis revealed 8 primary signaling pathways in "metabolism," 7 primary signaling pathways in "genetic information processing," 6 primary signaling pathways in "organismal systems," 4 primary signaling pathways in "cellular processes," and 3 primary signaling pathways in "environmental information processing" (Table 6). "MAPK signaling pathway" (ko04010) enrichment was repressed ($q < 0.05$) in Schwann cells treated with cold-stimulated adipocyte supernatant (Fig. 6).

3.5. Validation of RNA-Seq data using RT-qPCR

To evaluate the changes in the Schwann cells treated with adipocyte supernatant at different temperatures, DEGs with a |log2 (Fold Change) | $\geq$ 1.5 and q-value (adjusted p-value) < 0.05 were defined as cold-responsive genes (Table 3–5). The GO analysis revealed that the DEGs were enriched in cell adhesion-related entries, and the most significantly expressed DEGs were selected for PCR validation (Fig. 7) to further verify the reliability of the sequencing results ($P < 0.0001$ [ANOVA] for protocadherin 9 [PCDH9] and intercellular adhesion molecule 1 [ICAM1]; $P = 0.1866$ [ANOVA] for melanoma cell adhesion molecule [MCAM]).

Compared to that in the 37 DMEM group, the relative mRNA expression of the adhesion molecules MCAM, PCDH9, and ICAM1 in the 37 ADIPO CM and 30 ADIPO CM groups exhibited a decreasing trend in response to treatment with adipocyte supernatant at different temperatures. This trend was also observed in the comparison between the 30 ADIPO CM and 37 ADIPO CM groups (Fig. 7A, B, and 7C), wherein the differences were statistically significant. The expression of three adhesion molecules (MCAM, PCDH9, and ICAM1) in the 30 ADIPO CM group

was the lowest, indicating that the expression of adhesion molecules in Schwann cells was significantly reduced in the supernatant of adipose cells at a low temperature. In the absence of the adipocyte supernatant, Schwann cells also exhibited lower expression of these molecules at a low temperature. This finding suggests that temperature changes can affect the expression of adhesion molecules in Schwann cells. In conclusion, adipocytes stimulated by low temperatures may secrete adipokines [17], which interfere with the function of adhesion molecules in Schwann cells.

4. Discussion

Bell's palsy is an acute idiopathic peripheral facial nerve palsy with an annual incidence of 15–20 per 100,000 individuals [19,20]. Although the etiology of Bell's palsy is unclear, environmental factors such as atmospheric pressure and drastic temperature changes may play a key role in the occurrence of Bell's palsy [1,7]. Adipocytes subjected to cold exposure exhibit upregulated inflammatory chemokine expression [17], which dysregulates the adipose tissue immune microenvironment, resulting in possible pathological changes in the myelin sheath. In the present study, we aimed to explore the effect of cold-exposed adipocytes (adipokines) on Schwann cell adhesion factors. Given that rats have little facial subcutaneous adipose tissue, adipocytes derived from inguinal subcutaneous white adipose tissue was used in the experiments, because the subcutaneous white adipose tissue does not differ morphologically or functionally throughout the body of rats.

Among the four groups, the 37 ADIPO CM group was used to simulate the effect of adipokines in adipose supernatant on facial nerve myelin sheath under normal body temperature, forming a stable facial nerve microenvironment. The 30 ADIPO CM group was used to simulate the effect of adipokines in adipose supernatant on facial nerve myelin sheath under a low temperature environment. In addition, the 37 DMEM and 30 DMEM groups were set up to explore the possible effect of direct temperature changes on facial nerves.

Cell adhesion molecules (CAM) are involved in a series of important physiological and pathological processes, including signal transduction and the immune response [21]. In Schwann cells, CAMs are also involved in the regulation of cell-cell junctions, which are key to the structure and function of myelin. Abnormal myelin function may occur when the genes involved in cell-cell junction regulation are dysregulated, with potential pathological results [22]. The Schwann cell microenvironment is in a dynamic balance [23]. Abnormal conditions, such as cold stimulation, can upset local homeostasis, disrupting the function of intracellular junctions and myelin [24], resulting in the blockage of neural signal transduction.

ICAM1, a member of the immunoglobulin superfamily (IGSF), mediates intercellular adhesion reactions [25]. MCAM is a non-Ca^{2+}-dependent cell adhesion molecule that also belongs to the IGSF. The most important function of MCAM is mediation of cell adhesion, including contact among neighboring cells and between cells and the extracellular matrix. MCAM also regulates cytoskeletal rearrangements [26]. The downregulation of MCAM hinders cell adhesion and reduces intercellular homotypic adhesion. PCDH9 belongs to the non-clustered pro-calmodulin family. Similar to calmodulin, PCDH9 mediates cell adhesion [27,28]. PCDH9 also regulates a variety of effector molecules [29]. The DEG analysis in the present study showed that adipocytes subjected to cold stimulation repressed the expression of ICAM1, MCAM, and PCDH9 in Schwann cells and reduced intercellular adhesion between Schwann cells, probably triggering abnormal peripheral nerve fiber signaling and axonal regeneration occurrence.

Mitogen-activated protein kinases (MAPKs) are ubiquitously expressed in eukaryotic cells. They act as upstream signaling molecules of ICAM1 [30]. We, therefore, deduced that exposure to low temperatures caused a decrease in the expression of downstream adhesion molecules by affecting the MAPK signaling pathway. Extracellular stimulatory signals induce the phosphorylation of key protein targets,

activate signal transmission from the cell membrane to the nucleus, and mediate the regulatory network. MAPKs regulate various physiological activities, such as inflammation, apoptosis, oncogenesis, tumor cell invasion, and metastasis. The sequential activation of MAPK kinase kinase (MAPKKK) and MAPK kinase (MAPKK) ultimately leads to the activation of MAPK [31]. MAPK is involved in hypothermia regulation, and the MAPK signaling pathway is also closely associated with lipid metabolism [32]. The formation of nerve fiber myelin is regulated by growth factors, such as brain-derived neurotrophic factor (BDNF) and nerve growth factor (NGF) [33]. The KEGG pathway analysis in our study showed that DEGs in the 30 ADIPO CM group were enriched in "MAPK signaling pathway" (ko04010). Additionally, the expression of DEGs such as *BDNF* and *NGF* was downregulated, and the "MAPK signaling pathway" (ko04010) activity was repressed in Schwann cells treated with cold-stimulated adipocyte supernatant (P < 0.05) (Fig. 6). Therefore, hypothermic conditions may stimulate the secretion of adipokines, which inhibit the expression of adhesion molecules by suppressing MAPKKK-MAPKK-MAPK phosphorylation. The reduced adhesion between Schwann cells might damage the myelin structure and ultimately cause the onset of Bell's palsy. Further studies are needed to elucidate the mechanism of this effect.

In summary, in Schwann cells treated with the supernatant of cold-stimulated adipocytes, the expression of downstream adhesion factors (ICAM1, MCAM, and PCDH9) was reduced, likely via the downregulation of the MAPK signaling pathway. The weakened adhesion ability and subsequent disruption of Schwann cell structure might cause demyelinating lesions.

Nonetheless, this study and experiment have certain limitations, as the expression of ICAM1, MCAM and PCDH9 was not determined at the protein level. Further investigations will need to be conducted to establish the association between MAPK pathway downregulation and differential expression of adhesion factors, with the ultimate goal to identify targeted drugs for alleviating Bell's palsy. Furthermore, this treatment approach can be extended to peripheral nerve lesions, providing relief to patients suffering from peripheral neuropathy that cannot be completely cured. The findings of the present study might assist in further elucidation of the currently unknown pathogenesis of Bell's palsy.

Credit author statement

Tiefeng Zhang: Conceptualization, Methodology, Software, Investigation, Data curation, Writing - original draft. Yaxin Gan: Methodology, Software, Investigation, Data curation. Yulan Bai: Methodology, Software. Weijiang Hao: Methodology, Software, Ziqi Zeng: Methodology, Software. Feng Wu: Methodology, Software, Investigation, Data curation. Xianqi Li: Supervision, Resources, Conceptualization, Methodology, Writing - review & editing, Project administration, Visualization, Funding acquisition.

Ethics approval and consent to participate

The experimental design was approved by the Animal Experimentation Committee of the Stomatological Hospital of Shanxi Medical University.

Patient consent for publication

Not applicable.

Declaration of competing interest

None.

Data availability

Data will be made available on request.

References

[1] W. Zhang, L. Xu, T. Luo, F. Wu, B. Zhao, X. Li, The etiology of Bell's palsy: a review, Journal of neurology 267 (2020) 1896–1905, https://doi.org/10.1007/s00415-019-09282-4.

[2] D. Savadi-Oskouei, A. Abedi, H. Sadeghi-Bazargani, Independent role of hypertension in Bell's palsy: a case-control study, Eur. Neurol. 60 (2008) 253–257, https://doi.org/10.1159/000151701.

[3] M. Riga, G. Kefalidis, V. Danielides, The role of diabetes mellitus in the clinical presentation and prognosis of Bell palsy, J. Am. Board Fam. Med. : JABFM 25 (2012) 819–826, https://doi.org/10.3122/jabfm.2012.06.120084.

[4] S.Y. Kim, D.J. Oh, B. Park, H.G. Choi, Bell's palsy and obesity, alcohol consumption and smoking: a nested case-control study using a national health screening cohort, Sci. Rep. 10 (2020) 4248, https://doi.org/10.1038/s41598-020-61240-7.

[5] P. Franzke, A. Bitsch, M. Walther, et al., Weather, weather changes and the risk of Bell's palsy: a multicenter case-crossover study, Neuroepidemiology 51 (2018) 207–215, https://doi.org/10.1159/000492671.

[6] P. Kokotis, S. Katsavos, Effects of wind chill factor, temperature and other meteorological parameters on the incidence of Bell's palsy: results based on a retrospective, 7-year long, Greek population study, Neuroepidemiology 45 (2015) 44–49, https://doi.org/10.1159/000433542.

[7] H. Zhao, X. Zhang, Y.D. Tang, J. Zhu, X.H. Wang, S.T. Li, Bell's palsy: clinical analysis of 372 cases and review of related literature, Eur. Neurol. 77 (2017) 168–172, https://doi.org/10.1159/000455073.

[8] E.M. Khedr, G. Fawi, M.A. Abbas, N.A. El-Fetoh, A.F. Zaki, A. Gamea, Prevalence of Bell's palsy in qena governorate, Egypt, Neurol. Res. 38 (2016) 663–668, https://doi.org/10.1080/01616412.2016.1190121.

[9] S. Nishiguchi, J. Branch, T. Tsuchiya, R. Ito, J. Kawada, Guillain-barré syndrome: a variant consisting of facial diplegia and paresthesia with left facial hemiplegia associated with antibodies to galactocerebroside and phosphatidic acid, The American journal of case reports 18 (2017) 1048–1052, https://doi.org/10.12659/ajcr.904925.

[10] A. Greco, A. Gallo, M. Fusconi, C. Marinelli, G.F. Macri, M. de Vincentiis, Bell's palsy and autoimmunity, Autoimmun. Rev. 12 (2012) 323–328, https://doi.org/10.1016/j.autrev.2012.05.008.

[11] L. Montani, J.A. Pereira, C. Norrmén, et al., De novo fatty acid synthesis by Schwann cells is essential for peripheral nervous system myelination, The Journal of cell biology 217 (2018) 1353–1368, https://doi.org/10.1083/jcb.201706010.

[12] S. Schmitt, L.C. Castelvetri, M. Simons, Metabolism and functions of lipids in myelin, Biochim. Biophys. Acta 1851 (2015) 999–1005, https://doi.org/10.1016/j.bbalip.2014.12.016.

[13] S. Bolívar, X. Navarro, E. Udina, Schwann cell role in selectivity of nerve regeneration, Cells 9 (2020), 2131, https://doi.org/10.3390/cells9092131.

[14] S. Basak, D.J. Desai, E.H. Rho, R. Ramos, P. Maurel, H.A. Kim, E-cadherin enhances neuregulin signaling and promotes Schwann cell myelination, Glia 63 (2015) 1522–1536, https://doi.org/10.1002/glia.22822.

[15] M.K. Piya, P.G. McTernan, S. Kumar, Adipokine inflammation and insulin resistance: the role of glucose, lipids and endotoxin, J. Endocrinol. 216 (2013) T1–t15, https://doi.org/10.1530/JOE-12-0498.

[16] H. Cao, Adipocytokines in obesity and metabolic disease, J. Endocrinol. 220 (2014) T47–T59, https://doi.org/10.1530/JOE-13-0339.

[17] W. Zhang, L. Xu, T. Luo, B. Zhao, F. Wu, X. Li, Immune-related gene expression profiles of hypothermia adipocytes for Bell's palsy: implications for Bell's palsy, Oral Dis. 25 (2019) 1652–1663, https://doi.org/10.1111/odi.13126.

[18] T. Schmittgen, Livak Kjnp, Analyzing real-time PCR data by the comparative C(T) method, Nat. Protoc. 3 (2008) 1101–1108, https://doi.org/10.1038/nprot.2008.73.

[19] S.H. Dong, A.R. Jung, J. Jung, et al., Recurrent Bell's palsy, Clin. Otolaryngol. : Off. J. ENT-UK ; Off.J. Netherlands Soc. Oto-Rhino-Laryngol.Cervico-Facial Surg. 44 (2019) 305–312, https://doi.org/10.1111/coa.13293.

[20] R.F. Baugh, G.J. Basura, L.E. Ishii, et al., Clinical practice guideline: Bell's palsy. Otolaryngology–head and neck surgery, Off.J. Am.Acad.Otolaryngol.Head Neck Surg. 149 (2013) S1–S27, https://doi.org/10.1177/0194599813505967.

[21] Z. Aktary, M. Alaee, M. Pasdar, Beyond cell-cell adhesion: plakoglobin and the regulation of tumorigenesis and metastasis, Oncotarget 8 (2017) 32270–32291, https://doi.org/10.18632/oncotarget.15650.

[22] T. Kodama, T.A. Marian, H. Lee, et al., MRTFB suppresses colorectal cancer development through regulating SPDL1 and MCAM, Proc. Natl. Acad. Sci. U. S. A. 116 (2019) 23625–23635, https://doi.org/10.18632/oncotarget.15650.

[23] A. Muscella, C. Vetrugno, L.G. Cossa, S. Marsigliante, TGF-β1 activates RSC96 Schwann cells migration and invasion through MMP-2 and MMP-9 activities, J. Neurochem. 153 (2020) 525–538, https://doi.org/10.1111/jnc.14913.

[24] M. Su, S.H. Soomro, J. Jie, H. Fu, Effects of the extracellular matrix on myelin development and regeneration in the central nervous system, Tissue Cell 69 (2021), 101444, https://doi.org/10.1016/j.tice.2020.101444.

[25] T.M. Bui, H.L. Wiesolek, R. Sumagin, ICAM-1: a master regulator of cellular responses in inflammation, injury resolution, and tumorigenesis, J. Leukoc. Biol. 108 (2020) 787–799, https://doi.org/10.1002/JLB.2MR0220-549R.

[26] D. Liu, L. Du, D. Chen, et al., Reduced CD146 expression promotes tumorigenesis and cancer stemness in colorectal cancer through activating Wnt/β-catenin signaling, Oncotarget 7 (2016) 40704–40718, https://doi.org/10.18632/oncotarget.9930.

[27] S. Strehl, K. Glatt, Q.M. Liu, H. Glatt, M. Lalande, Characterization of two novel protocadherins (PCDH8 and PCDH9) localized on human chromosome 13 and mouse chromosome 14, Genomics 53 (1998) 81–89, https://doi.org/10.1006/geno.1998.5467.

[28] R.S. Bradley, A. Espeseth, C. Kintner, NF-protocadherin, a novel member of the cadherin superfamily, is required for Xenopus ectodermal differentiation, Curr. Biol. : CB 8 (1998) 325–334, https://doi.org/10.1016/s0960-9822(98)70132-0.

[29] C. Shi, Y. Yang, L. Zhang, et al., MiR-200a-3p promoted the malignant behaviors of ovarian cancer cells through regulating PCDH9, OncoTargets Ther. 12 (2019) 8329–8338, https://doi.org/10.2147/OTT.S220339.

[30] P. De Cesaris, D. Starace, G. Starace, A. Filippini, M. Stefanini, E. Ziparo, Activation of Jun N-terminal kinase/stress-activated protein kinase pathway by tumor necrosis factor alpha leads to intercellular adhesion molecule-1 expression, J. Biol. Chem. 274 (1999) 28978–28982, https://doi.org/10.1074/jbc.274.41.28978.

[31] Y. Sun, W.Z. Liu, T. Liu, X. Feng, N. Yang, H.F. Zhou, Signaling pathway of MAPK/ERK in cell proliferation, differentiation, migration, senescence and apoptosis, J. Recept. Signal Transduct. Res. 35 (2015) 600–604, https://doi.org/10.3109/10799893.2015.1030412.

[32] J.R. Broatch, A. Petersen, D.J. Bishop, Postexercise cold water immersion benefits are not greater than the placebo effect, Med. Sci. Sports Exerc. 46 (2014) 2139–2147, https://doi.org/10.1249/MSS.0000000000000348.

[33] A.E. Mortimer, A. Faroni, M.A. Kilic, A.J. Reid, Maintenance of a schwann-like phenotype in differentiated adipose-derived stem cells requires the synergistic action of multiple growth factors, Stem Cell. Int. 2017 (2017), 1479137, https://doi.org/10.1155/2017/1479137.